Importance of Kinetics in Surface Alloying: A Comparison of the Diffusion Pathways of Pd and Ag Atoms on Cu(111)

ARTICLE *in* THE JOURNAL OF PHYSICAL CHEMISTRY C · JULY 2009

Impact Factor: 4.77 · DOI: 10.1021/jp903541k

6 AUTHORS, INCLUDING:

Jeong Woo Han
University of Seoul
37 PUBLICATIONS **395** CITATIONS
SEE PROFILE

Heather L. Tierney
American Chemical Society
37 PUBLICATIONS **658** CITATIONS
SEE PROFILE

Ashleigh Baber
James Madison University
44 PUBLICATIONS **891** CITATIONS
SEE PROFILE

Charles Sykes
Tufts University
113 PUBLICATIONS **1,708** CITATIONS
SEE PROFILE

Importance of Kinetics in Surface Alloying: A Comparison of the Diffusion Pathways of Pd and Ag Atoms on Cu(111)

Darin O. Bellisario,[†] Jeong Woo Han,[‡] Heather L. Tierney,[†] Ashleigh E. Baber,[†] David S. Sholl,[‡] and E. Charles H. Sykes*,[†]

Department of Chemistry, Tufts University, Medford, Massachusetts 02155-5813, and School of Chemical and Biomolecular Engineering, Georgia Institute of Technology, 311 Ferst Drive, Atlanta, Georgia 30332-0100

Received: April 17, 2009; Revised Manuscript Received: June 2, 2009

The microscopic details of how metals alloy have important consequences for both their material properties and their chemical reactivity. In this study, the initial stages of alloying of Pd and Ag with Cu(111) are compared. Low-temperature scanning tunneling microscopy reveals that physical vapor deposition of Pd and Ag at or above room temperature yields remarkably different surface alloys: Pd predominantly incorporates at the nearest ascending Cu step edge, whereas Ag appears to be able to traverse step edges rather easily and alloys into terraces both above and below its initial adsorption site. Density functional theory calculations reveal that even though Pd adatoms have a lower barrier than Ag for traversing step edges, unlike Ag they bind very strongly to ascending step edges and remain there permanently. This leads to a situation in which Pd atoms have at most a very small number of attempts to leave the terrace on which they are deposited before they are incorporated into the nearest ascending step edge. Ag adatoms, however, have many opportunities to cross step edges and can alloy at positions far from their initial starting point. This direct comparison demonstrates the importance in combining theory and experiment in order to understand complicated surface alloying mechanisms and illustrates how both the kinetics and the thermodynamics of the process must be considered to fully understand experimental observations.

Introduction

The unique properties of bimetallic alloys have played a major role in heterogeneous catalysis for decades. The tunability offered by mixing different elements with control over stoichiometry allows catalysts to be made with greater activity, selectivity, and stability than those derived from single metals. Understanding the atomic-scale surface structure of alloys is a crucial step on the path toward designing optimal heterogeneous catalysts. Only fairly recently has the nanoscale surface structure of metal alloys begun to be reported.[1−11] The two alloy systems of direct relevance to this article are Ag/Cu(111) and Pd/Cu(111). Pd/Cu alloys are an important class of materials used for hydrogen purification membranes and also serve as the active metals in many heterogeneous catalysts.[12−16] Because of the technological importance of Pd/Cu alloys, a wide variety of experimental and theoretical studies have been performed in order to uncover the surface physics and chemistry of these systems.[4,17−29] The bulk alloys exist in both ordered and disordered phases; however, at most catalytically relevant temperatures and compositions the binary Pd−Cu system is a disordered fcc alloy.[4,30−32] Surface studies have shown that the top atomic layer of Pd/Cu alloys is rich in Cu, whereas the near-surface region (∼7 atomic layers) is rich in Pd.[33] However, if there are strongly interacting adsorbates present, Pd is brought to the surface.[34] Aaen et al. used scanning tunneling microscopy (STM) to study the structure of surface alloys formed by physical vapor deposition of Pd onto Cu(111) at a variety of temperatures.[4] They found that after deposition, the Pd was incorporated into the surface via ascending step edges and that the width of the Cu/Pd alloy brims, which formed above the Cu step edges, was dependent in size on the lower terrace.

There has also been much recent interest in Ag/Cu alloys for catalytic applications. For example, both theory and experiments have focused on Ag/Cu alloys as improved catalysts for ethylene epoxidation.[35,36] Several surface science and theoretical studies have unraveled the complex surface structures formed when Ag is deposited onto Cu(111).[5,6,37−40] Bendounan et al. demonstrated that the simplest case occurs below room temperature when Ag forms an incommensurate layer on top of the Cu(111) surface.[5] This overlayer appeared as a Moiré pattern in STM images due to the mismatch of Ag and Cu atom diameters (bulk $d_{Cu} = 0.256$ nm; bulk $d_{Ag} = 0.289$ nm).[5] At and above room temperature, the situation is more complex as deposition of a single atomic layer of Ag reconstructs the Cu substrate directly beneath it.[5,6,37−40] The mismatch between the Cu(111) surface and the overlayer of larger Ag atoms strains the surface. This instability makes it energetically favorable for the Cu surface layer to expel atoms and reorganize into regularly spaced triangular hcp packed domains surrounded by unreconstructed fcc domains. The resulting alloy contains a regular array of triangular regions wherein the three topmost Cu layers adopt an hcp configuration.[5,6,37−40]

In this article, we compare and contrast how the initial stages of alloying occur in both Pd/Cu(111) and Ag/Cu(111) systems. STM and DFT studies are combined in order to understand how alloying proceeds and to quantify the energetics of the diffusion pathways of Pd and Ag atoms on Cu(111).

Experimental Section

I. Experimental Methods. All STM experiments and sample preparation described in this work were performed within an

* To whom correspondence should be addressed. E-mail: charles.sykes@tufts.edu.
[†] Tufts University.
[‡] Georgia Institute of Technology.

10.1021/jp903541k CCC: $40.75
Published on Web 06/25/2009

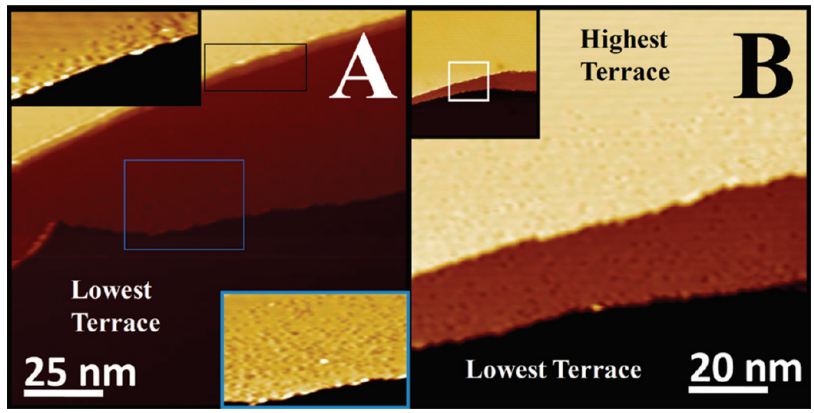

Figure 1. STM images of 0.01 ML Pd/Cu(111) deposited at a temperature of 435 K. (A) Upon diffusing to an ascending Cu step edge, Pd atoms alloy into the upper terrace. The widths of the Pd brims in this image are proportional to the size of the lower terrace. The presence of a small terrace in the middle of the image leads to a narrower brim on the upper part of the highest terrace as compared to the wider brim above the large lowest terrace. When comparably sized terraces are involved, the width of the resulting Pd brim is always dependent on the size of the lower terrace. (B) When the upper terrace is significantly larger than the lower terrace, however, unusually large brims are observed at the edge of the upper terrace as seen in this figure. The inset shows an expanded image of the same area of the surface and reveals that the upper and lower terraces are indeed much larger than the terrace of intermediate height. The brim on the small intermediate terrace is large because the lower terrace is large; however, the brim on the upper terrace is large because the upper terrace itself is large, as seen in the inset. This new finding that the upper terrace has an unusually large Pd brim is attributed to a secondary mechanism that operates on large terraces in which more Pd atoms attempt to cross down the Ehrlich−Schwoebel barrier of the descending step. Image conditions: (A) $I = 0.1$ nA and $V = -0.4$ V; (B) $I = 0.1$ nA and $V = 0.5$ V.

ultrahigh vacuum chamber with pressures lower than 5×10^{-10} mbar. The Cu(111) surface (MaTecK) was prepared at room temperature by cycles of Ar^+ sputtering (1.0 keV/18 μA) for 30 min followed by a 2 min anneal to 820 K. Approximately 12 of these sputter/anneal cycles were performed upon receiving the crystal, followed by a further 2 sputter/anneal cycles between each STM experiment. After cooling the Cu(111) sample, Ag or Pd was added by vapor deposition via the resistive heating of a Ag- or Pd-wrapped W wire at a rate of 0.01 ML/min. The Pd and Ag sources were calibrated by analysis of many atomically resolved STM images. After Ag deposition, the crystal was transferred in less than 5 min in vacuum ($<5 \times 10^{-10}$ mbar) to the precooled STM. In approximately 30 min, the sample cooled from room temperature to 78 K, at which temperature all STM images are taken. All images were recorded with etched W tips, and voltages refer to the sample bias.

II. Computational Methods. Plane wave DFT calculations have been performed using the Vienna *ab initio* simulation package (VASP) with the ultrasoft pseudopotentials available in this package.[41,42] In all calculations, we have used the generalized gradient approximation (GGA) with the Perdew−Wang 91[43] functional and a plane wave cutoff energy of 241.6 eV. The geometries of the structures in our calculations were relaxed using a conjugate gradient algorithm until the forces on all the unconstrained atoms were less than 0.03 eV/Å. In order to represent the diffusion of an adatom at the stepped and kinked sites on Cu, we have used Cu(322) and Cu(643) surfaces, respectively. Cu(322) has steps with {100} microfacets on a (111) terrace, while Cu(643) has steps with both {100} and {110} microfacets on a (111) terrace; therefore, these two steps are representative of the full range of step orientations that can exist on a (111) terrace. A $2 \times 5 \times 1$ *k*-point mesh was used for the (322) surfaces with a (3×1) surface unit cell and a $3 \times 3 \times 1$ *k*-point mesh for the (643) surfaces with a (1×1) surface unit cell. The surface unit cells were defined using the DFT-optimized Cu lattice constant, and the slab thickness for each surface was ~10.5 Å separated by a vacuum spacing of ~14 Å in the direction of the surface normal. No atoms were constrained during calculations with these supercells.

The nudged elastic band (NEB) method has been employed to investigate diffusion pathways of adatoms on those surfaces.[44,45] Initial approximations to reaction paths were obtained by linear interpolation between energy minima. The same set of *k*-points and energy cutoff were used for NEB calculations as were mentioned above. The total number of intermediate images we used for Figures 4, 5, and 6 was 18, 22, and 19, respectively, which is sufficient to map the minimum energy path (MEP) accurately. In Figures 4−6, we denote the net reaction coordinates by defining a straight line between the initial and final position of the diffusing atom in the plane of the surface and projecting the full coordinates of each NEB image onto that line.

Results

STM of Pd/Cu(111). STM images of surface alloys formed when low coverages of Pd (0.01 ML) were deposited on the Cu(111) surface are shown in Figure 1. The Pd atoms were found to incorporate into Cu terraces at ascending step edges, forming a brim of Pd atoms. A brim is an area in which Pd is substitutionally alloyed in both the surface and subsurface sites of the Cu crystal. These brims lack any global order but have previously been shown to be stable well above room temperature (≥600 K) due to long-range Pd−Pd interactions that are optimized when no nearest neighbor Pd−Pd pairs are present.[4] From an inspection of Figure 1, it is clear that the width of the Pd brims varies depending on the surface morphology. Aaen et al. observed that the width of the brim above a step edge was dependent on the size of the terrace below the step edge so that the larger the lower terrace, the wider the Pd brim on the upper terrace.[4] Conversely, the same group found that no correlation existed between the width of a Pd brim and the size of the terrace on which the brim is formed.[4] This result is reflected in Figure 1A, where the width of the Pd brims is proportional to the size of the lower terraces. Aaen et al. explained these findings with a proposed mechanism involving Pd adatoms incident upon a terrace migrating to the nearest ascending step edge and alloying into the terrace above that step via step fluctuations and vacancy mediated diffusion.[2,4] The data in Figure 1 were recorded after

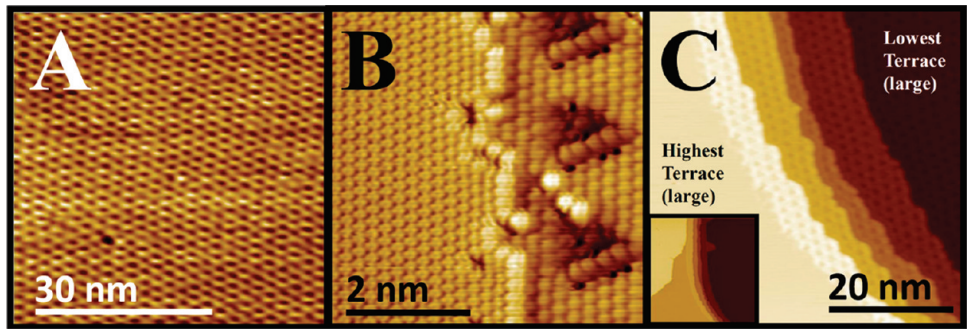

Figure 2. STM images of 0.7 ML of Ag on Cu(111) deposited at a temperature of 300 K. (A) Large scale image showing a large Cu terrace completely covered with a monolayer of Ag. (B) Atomic resolution of the interface between a Cu(111) terrace and a Ag monolayer that has nucleated and grown from a descending step. (C) A large scale image that reveals that smaller terraces, even in series, tend to fill with Ag faster than larger ones. The inset shows a zoomed out image of the same region. This phenomenon suggests that Ag does, to a significant extent, cross Cu step edges at 300 K. Image conditions: (A) $I = 0.05$ nA and $V = 0.6$ V; (B) $I = 0.55$ nA and $V = 1.0$ V; (C) $I = 0.05$ nA and $V = 0.6$ V.

Pd was deposited on Cu(111) at 435 K. Additional experiments in which low coverages of Pd were deposited at temperatures between 300−500 K yielded the same result that Pd appears in brims above ascending step edges and that only the ratio of surface to subsurface Pd varies as a function of temperature.[4,29] This point becomes salient later in the article when the initial stages of Pd alloying on Cu(111) is compared with Ag.

Our results verify this phenomenon but with an additional important consideration. While adjacent terraces of similar sizes behave according to this model, we have observed that larger terraces above much smaller terraces have unusually large Pd brims, as shown in Figure 1B. In this case, according to the mechanism proposed by Aaen et al., deposition of a low coverage of Pd onto the Cu(111) surface would not provide a sufficient amount of Pd to the small terrace seen at the center of Figure 1B to form the large Pd brim that is seen on the ascending terrace. This brim is roughly the same width as the brim at the edge of the small terrace, which is composed of all the Pd from the large lower terrace. These new results suggest that in addition to the accepted mechanism of Pd incorporation via diffusion to ascending step edges[4] there is an additional mechanism in operation that allows large terraces to supply Pd to their own brim. This point will be addressed at length in the Discussion section.

STM of Ag/Cu(111). Even at first inspection, Ag behaves in a manner very different from that of Pd when deposited on Cu(111). Previous work has shown that at room temperature, deposition of a single atomic layer of Ag reconstructs the Cu substrate directly beneath it.[5,6,37−40] The presence of 1 ML of Ag causes the Cu layer directly underneath to expel atoms and reorganize into regularly spaced triangular hcp packed domains surrounded by unreconstructed fcc domains. Figure 2A is a large scale image of this reconstruction in which a single terrace is covered in a hexagonal array of small triangles (spacing 2.6 nm) that result from the reconstruction of the Cu layer. Figure 2B is a high-resolution image of three of these triangles at the interface between the edge of the Ag layer and what was a Cu step edge prior to Ag deposition. The Ag layer seen in the right side of the image has grown on a lower Cu terrace and therefore is only very slightly higher (0.01 nm) than the upper Cu(111) terrace on the left. Careful inspection of Figure 2B also reveals that the Ag atoms ($d_{Ag} = 0.289$ nm) of the layer on the right side of the image are slightly larger than the Cu atoms ($d_{Cu} = 0.256$ nm) of the bare Cu(111) terrace on the left. Figure 2C shows the most striking difference between how Ag and Pd interact with Cu(111). It is clear from Figure 2C that the three small terraces running vertically at the center of the image are completely covered by Ag, whereas the much larger lowest and highest terraces are mostly free of Ag. This is in stark contrast to what would be observed with Pd; one would expect that a large brim would be formed above the larger lowest terrace and that a negligible amount of metal would have collected on the staircase of smaller terraces. These observations suggest that, unlike Pd on Cu(111), during the alloying process, a significant population of Ag adatoms must cross step edges.

The higher coverage data presented in Figure 2 reveals some important features of how Ag nucleates on Cu(111) and hints that it behaves in a manner different from that of Pd. However, in order to make a direct comparison of these two systems, alloying data of similar coverages must be compared. The fact that Ag and Pd atoms are larger than the surface Cu atoms and electronically different allowed individual Ag or Pd atoms in the surface and subsurface layers to be identified in STM images.[4] Figure 3A shows that when low coverages of Ag are deposited at 330 K, Ag actually behaves in a manner similar to that of Pd (Figure 3B) in that it forms brims at the step edges which consist of single Ag atoms substituted into the surface layer of Cu atoms. However, an important difference between Pd and Ag alloying is observed in Figure 3A, which shows that comparable quantities of Ag alloy near both the ascending (I) and the descending (II) step edges. The Ag brim labeled (II) has formed above the lowest terrace and presumably consists of Ag that was incident on the lowest terrace. The band of bare Cu between these brims suggests that the brim near the ascending step edge (I) consists of Ag adatoms that were initially incident upon the highest terrace. In contrast, Figure 3B shows that under the same conditions Pd forms a significantly larger brim (IV) at the descending step edge above the lower terrace, with only very few scattered Pd atoms alloyed in the middle terrace below the ascending step edge (III).

Theory. To enhance our understanding of the complex alloying behavior exhibited by Ag and Pd, DFT calculations were performed. The STM results suggested that in the case of Ag, adatoms crossed step edges during the process of alloying. In contrast, Pd adatoms were mostly incorporated into the nearest ascending step edge, unless very wide terraces were involved. To explore these observations with DFT, diffusion barriers for Ag and Pd on Cu(111) were calculated both on the flat terraces and for a variety of step edge types. Diffusion pathways of Ag (A) and Pd (B) on Cu(322) are shown in Figures 4 and 5. The energy of the initial configuration, corresponding to the adatom in an fcc hollow site close to the upper step edge on this stepped surface, was defined to be zero for each set of calculations. It is known that there are two possible diffusion

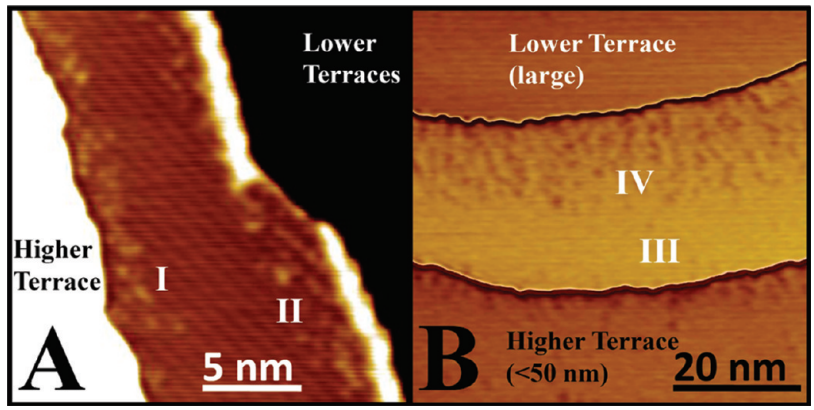

Figure 3. Comparison of Ag and Pd alloying mechanisms in Cu(111). (A) STM image of Ag on Cu(111) deposited at 330 K with image contrast such that Ag incorporated in the central terrace can be seen. It is clear that Ag atoms alloy into the Cu(111) surface both above (II) and below (I) step edges. The higher terrace in the image is large, and the lower terrace is small (<20 nm) (B) In contrast, Pd deposition results in surface alloy formation almost exclusively on the upper terraces of steps (IV) with very limited alloy growth below steps (III). Image conditions: (A) $I = 1$ nA and $V = 0.9$ V; (B) $I = 0.50$ nA and $V = -0.6$ V.

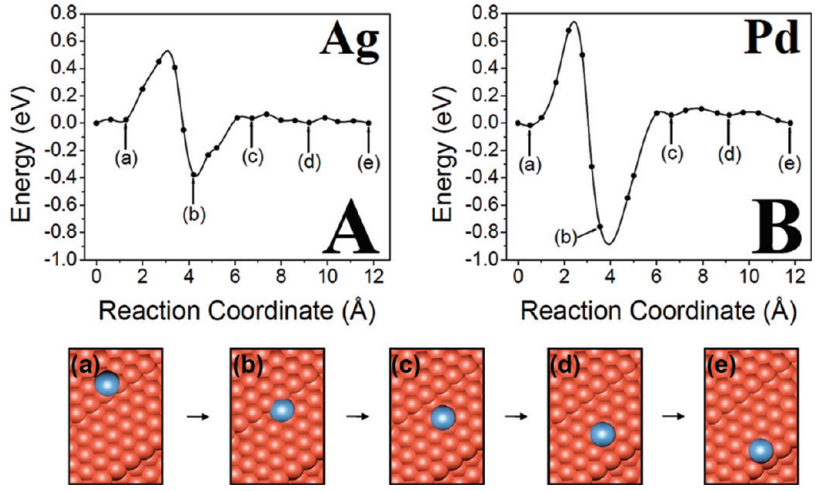

Figure 4. Nudged elastic band results for the diffusion of Ag (A) and Pd (B) on Cu(322) by a hopping mechanism. The energy of the adatom on the lower terrace away from the step edge (final position) is the same as the starting point on the upper terrace (initial position). DFT predicts that the Ehrlich−Schwoebel barrier at the Cu(322) step edge is 0.45 eV for Ag and 0.68 eV for Pd.

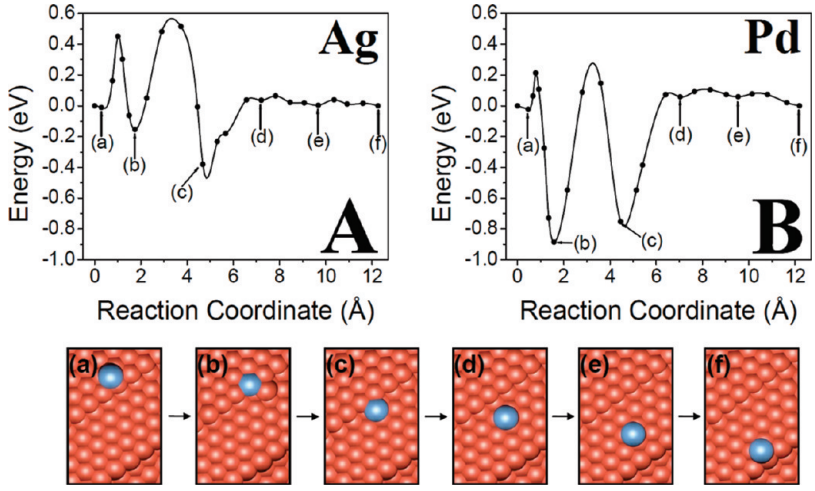

Figure 5. Nudged elastic band results for the diffusion of Ag (A) and Pd (B) on Cu(322) by an exchange mechanism. The energy of the adatom on the lower terrace away from the step edge (final position) is the same as the starting point on the upper terrace (initial position). The Ehrlich−Schwoebel barriers on the step edge are 0.45 eV (A) and 0.21 eV (B). Unlike the hopping mechanism, a second barrier (step b to c) must be overcome in order to fully clear the step edge.

mechanisms for adatom motion across a step edge: hopping and exchange.[46,47] Both cases have been examined in order to investigate which mechanism is more favorable in this system. The diffusion of the adatom via the hopping (exchange) mechanism is plotted in Figure 4 (Figure 5). The results shown in Figure 4 reveal that adatom diffusion across the step via a

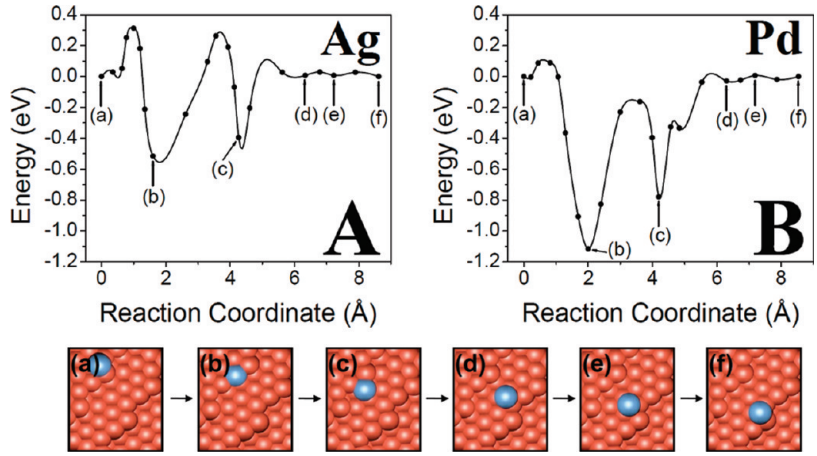

Figure 6. Nudged elastic band results for the diffusion of Ag (A) and Pd (B) on Cu(643) by an exchange mechanism. The energy of the adatom on the lower terrace away from the step edge (final position) is the same as the starting point on the upper terrace (initial position). The Ehrlich−Schwoebel barriers were calculated to be 0.31 eV (A) and 0.09 eV (B). The second energetic barrier occurs when the adatom moves out of the step edge (step b to c).

hopping mechanism involves an Ehrlich−Schwoebel (ES) barrier[48] of 0.45 eV (0.68 eV) for Ag (Pd). After crossing the step, the adatom is in a more coordinated site (b in Figure 4) compared with its initial site on a terrace (a in Figure 4). Because of its higher coordination, site b is the most stable site in the diffusion pathway for hopping over a step edge that we examined. In order for a Ag (Pd) adatom to escape from site b, an energy of ∼0.4 eV (∼0.8 eV) is required. In moving from c to d to e in Figure 4, an adatom diffuses away on the terrace and arrives at an energetically equivalent site to the starting point but on the lower terrace. This cycle would then be repeated if an adatom diffused down another step.

In contrast to hopping, for the diffusion via an exchange mechanism the diffusing adatom must undergo two separate processes to get to a point equivalent to position b in Figure 4. First, the adatom displaces a step edge Cu atom beneath it and assumes its position (step a to b in Figure 5). Then, the adatom diffuses out toward the lower terrace, and the displaced Cu atom returns to its original position (step b to c in Figure 5). The Ehrlich−Schwoebel barriers during this process, that is, the diffusion barrier from a to b in Figure 5, are 0.45 eV (0.21 eV) for Ag (Pd). In order for an Ag (Pd) adatom to diffuse from b to c in Figure 5, an energy barrier of 0.67 eV (1.04 eV) must be overcome. Once the adatom arrives at c in Figure 5, the remainder of the pathway is the same as that in the hopping mechanism. Thus, the pathway from c to e in Figure 4 is equivalent to that from d to f in Figure 5. Comparing the Ehrlich−Schwoebel barriers via both mechanisms, we see that the barrier is the same for Ag adatoms, but the exchange mechanism is more favorable for Pd adatoms.

While Cu(322) is a reasonable model for understanding the diffusion of adatoms across step edges, the shape of Cu step edges at room temperature is in constant flux.[49−54] For this reason, DFT calculations were performed for the exchange mechanism occurring at kink sites. Because the Ehrlich−Schwoebel barrier for the exchange mechanism is much lower than the hopping mechanism for Pd on Cu(322), only the exchange mechanism was investigated for this case. As can be seen in Figure 6, the starting point for the adatom is on an fcc hollow site just above the kink site. This diffusion path also has two stages. From a to b in Figure 6, the adatom displaces the Cu kink site atom and assumes the Cu atom's original position. During this process, the Ehrlich−Schwoebel barrier for an Ag (Pd) adatom was 0.31 eV (0.09 eV). Then, from b to c, the displaced Cu atom assumes its original position, and the adatom moves onto the lower terrace. The energy barrier of this process was found to be 0.78 eV (0.96 eV) for the Ag (Pd) adatom. Similar to the situation for Cu(322), in order for an adatom to move away from the step, i.e., from c to d, an energy of ∼0.4 eV (∼0.8 eV) is needed because c is the more coordinated, stable site. From d to f in Figure 6, the adatom diffuses away on the terrace and arrives at a site equivalent to the starting point, but on the lower terrace. Similar to the exchange mechanism on Cu(322), the Ehrlich−Schwoebel barrier of Ag was found to be 0.22 eV larger than that of Pd. Interestingly, it has been observed experimentally in the case of Mn on Cu(100) that the amount of alloy formation in lower terraces can be correlated with the kink density at steps.[55] Our DFT results provide an example of how this observation can arise and suggest that the barrier for incorporating into the lower step edge at kink sites is ∼0.1 eV lower than that on straight step edges for both Pd and Ag.

Discussion

By directly comparing the alloying of low concentrations of Pd and Ag in Cu(111) with STM, we have observed several important differences. It appears that the main mechanism for Pd incorporation in the surface is alloying into ascending step edges. Only when very large terraces are involved does any Pd become incorporated below the step edges. In contrast, Ag alloys both above and below step edges. In order to quantify the energetics of the initial stages of alloying, DFT calculations were performed on both stepped and kinked Cu surfaces. The DFT calculations confirm that there are several available pathways by which adatoms can either cross step edges or become incorporated into the step edges themselves. While we have presented the progression of an adatom across and/or into a step edge, microscopic reversibility allows us to examine exactly the same energetics for the reverse process, i.e., an adatom approaching a step edge from the lower terrace and either alloying into it or hopping onto the upper terrace.

The first important point that emerges from our calculations is that for all three mechanisms studied (hopping, exchange at straight steps, and exchange at kinked steps) the potential wells are deeper for Pd than for Ag. For example, a Pd atom is ∼0.8 eV more stable when coordinated to a step edge relative to the most stable site on a flat terrace (Figures 4B, 5B, and 6B). In

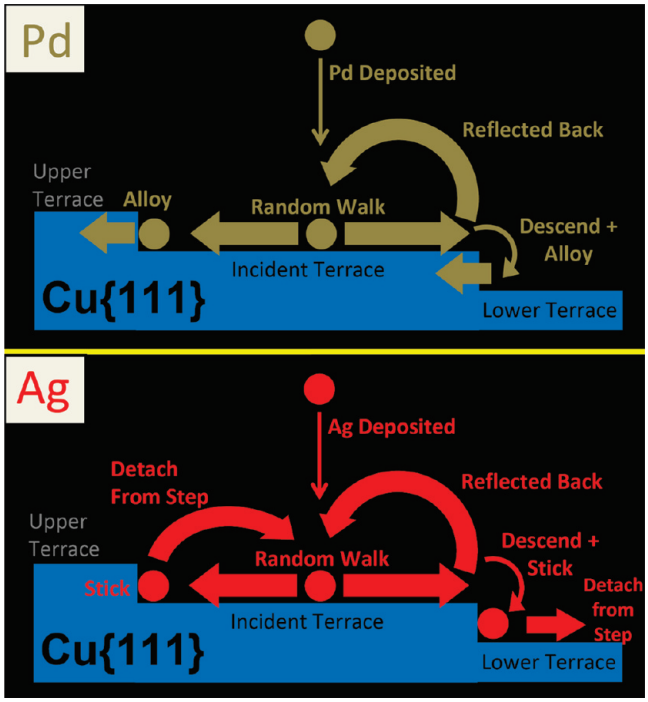

Figure 7. Schematic of the proposed mechanism of Ag and Pd alloying with Cu(111). The thickness of the arrows indicates the relative number of events. Pd atoms bind irreversibly to ascending step edges and hence have at most only a very small number of chances to cross to the lower terrace. The crossing process, unlike binding to ascending step edges, is activated, and hence, most atoms are reflected back onto the terrace. In contrast, Ag binds more weakly to ascending step edges and can have multiple attempts to cross step edges.

contrast, the same energy difference for Ag is only ~0.4 eV. This large difference means that, unlike Ag, once Pd becomes associated with a step edge it is unlikely to leave it. At 300 K (assuming a pre-exponential factor of 10^{12}), a Ag adatom would have an average residence time at the step edge of ~5 μs as compared with Pd's residence time of ~28 s. This long residence time for Pd atoms at step edges means that once they contact their nearest ascending step edge they remain there on a long time scale and are presumably incorporated further into the brim of the step edge via step fluctuations and vacancy mediated diffusion.[2,4,49−55] Ag, however, can bind and detach from a step with great frequency during the alloying process because of its weaker binding to step edges.

Figure 7 shows a schematic of the proposed alloying process for both Pd and Ag atoms. After evaporation, the metal atoms diffuse randomly over the terrace they initially land on. If Pd encounters an ascending step edge, it remains there and is incorporated in the brim via step fluctuations and vacancy mediated diffusion.[2,4,49−55] However, Ag can fairly easily detach from ascending step edges and diffuse back onto the terrace. During their random walk, Pd and Ag atoms will also encounter descending step edges. Unlike binding to ascending step edges, traversing descending step edges is an activated process (see Figures 4−6). Therefore, depending on the barrier height, some diffusing adatoms may occasionally cross down step edges, while most are reflected back onto the terrace. Of the three mechanisms we have considered, the lowest barrier available to Ag is to traverse a descending step edge via the exchange mechanism at a kink site (0.3 eV, Figure 6A). Crossing this barrier leads to an end point at which the adatom is incorporated into the lower step edge. Figure 5 reveals that a similar process for Ag at a straight step would have a slightly higher barrier of 0.4 eV. In contrast, both of these mechanisms for step crossing offer Pd an even lower energy barrier: 0.2 eV for exchange at the straight step and 0.1 eV for the kinked step.

From these results, one would naively expect to observe more Pd to accumulate below step edges; however, both the average residence times at ascending step edges and the probability of crossing descending step edges must be taken into account to fully understand the situation. While Pd is more likely to cross down a descending step edge, it binds essentially irreversibly to ascending steps; this binding limits the number of attempts a Pd adatom makes at crossing a descending step edge to those attempts made before the binding event occurs. Conversely, Ag can bind and detach from ascending steps many times during the alloying process, and thus, each Ag atom will have many attempts at crossing descending step edges; this more than compensates for the higher reflection probability for Ag off of descending step edges. In a simplistic one-dimensional (1D) case, when Pd or Ag adatoms diffuse toward a descending step edge they are presented with two barriers: the diffusion barrier back onto the terrace or the Ehrlich−Schwoebel barrier for crossing down the step edge. Our DFT calculations reveal that the diffusion barriers on the Cu(111) terrace are small and almost the same for Ag (0.040 eV) and Pd (0.035 eV), whereas the Ehrlich−Schwoebel barriers via the lowest energy pathway are 0.3 eV for Ag and 0.1 eV for Pd. A simplistic Arrhenius rate calculation reveals that at room temperature the probability for a Pd atom to cross a step edge is ~5% vs 0.005% for an Ag atom. While the probability for Ag is much lower than that for Pd, the fact that Ag is relatively weakly bound to ascending step edges means that over the course of the alloying process (tens of minutes) the Ag adatoms have many attempts ($>10^8$) at crossing down step edges. While this 1D model of competing processes is simplistic, the very large differences in rates of the various processes for Ag and Pd are sufficient to explain the differences between the final alloying positions of Ag and Pd observed experimentally. The unusually large Pd brims we find at the edge of very large Cu(111) terraces can also be explained within this model. A large terrace will have a large number of Pd atoms incident upon it. Therefore, the large flux of Pd atoms incident upon the descending step will contribute to the formation of an unusually large brim. Additionally, the large spatial gap between the ascending and descending step edges of a large terrace increases the likelihood that adatoms reflected from the descending step will return before diffusing to the distant ascending step edge. While the experiments were performed at relatively low coverages and the DFT models considered just one atom, the processes at play (crossing the Ehrlich−Schwoebel barrier and exchanging into the step edge) are essentially the same regardless of coverage except that the energetics of each process will change slightly as the surface becomes more alloyed.

Conclusions

In this article, we have compared and contrasted how the initial stages of alloying occur in both Pd/Cu(111) and Ag/Cu(111) systems. Our results show that Pd and Ag behave very differently in the initial stages of alloying on Cu(111). Our data reveals how the Ehrlich−Schwoebel barrier at step edges affects the initial stages of surface alloy formation. It appears that the strong binding of Pd to ascending step edges leads to the incorporation of most of the Pd incident on a terrace in brims at the upper terraces. Ag, however, binds more weakly to these sites and hence has many opportunities to attempt to traverse the Ehrlich−Schwoebel barrier. These results have implications

for many alloy systems in which surface diffusion of the constituent metals is necessary for the particles to remain active and also for systems in which such diffusion is detrimental in terms of surface segregation of the inactive element.

Acknowledgment. We thank the NSF (Grant #0717978) for support of this research. E.C.H.S. thanks Research Corporation and the Beckman Foundation for additional support. D.O.B. thanks NSF for an REU fellowship. A.E.B. and H.L.T. thank the DOEd for GAANN fellowships. We are grateful to Andrew Gellman for helpful discussions of the data.

References and Notes

(1) Hebenstreit, E. L. D.; Hebenstreit, W.; Schmid, M.; Varga, P. *Surf. Sci.* **1999**, *441*, 441.
(2) Nagl, C.; Haller, O.; Platzgummer, E.; Schmid, M.; Varga, P. *Surf. Sci.* **1994**, *321*, 237.
(3) Schmid, M.; Stadler, H.; Varga, P. *Phys. Rev. Lett.* **1993**, *70*, 1441.
(4) Aaen, A. B.; Laegsgaard, E.; Ruban, A. V.; Stensgaard, I. *Surf. Sci.* **1998**, *408*, 43.
(5) Bendounan, A.; Cercellier, H.; Fagot-Revurat, Y.; Kierren, B.; Yurov, V. Y.; Malterre, D. *Phys. Rev. B* **2003**, *67*.
(6) Bendounan, A.; Cercellier, H.; Fagot-Revurat, Y.; Kierren, B.; Yurov, V. Y.; Malterre, D. *Appl. Surf. Sci.* **2003**, *212*, 33.
(7) Han, P.; Axnanda, S.; Lyubinetsky, I.; Goodman, D. W. *J. Am. Chem. Soc.* **2007**, *129*, 14355.
(8) Hwang, R. Q.; Bartelt, M. C. *Chem. Rev.* **1997**, *97*, 1063.
(9) Yuhara, J.; Schmid, M.; Varga, P. *Phys. Rev. B* **2003**, *67*, 1954071.
(10) Besenbacher, F.; Chorkendorff, I.; Clausen, B. S.; Hammer, B.; Molenbroek, A. M.; Norskov, J. K.; Stensgaard, I. *Science* **1998**, *279*, 1913.
(11) Han, J. W.; Kitchin, J. R.; Sholl, D. S. *J. Chem. Phys.* **2009**, *130*, 1247101.
(12) Anderson, J. A.; FernandezGarcia, M.; Haller, G. L. *J. Catal.* **1996**, *164*, 477.
(13) Choi, K. I.; Vannice, M. A. *J. Catal.* **1991**, *131*, 36.
(14) Ma, Y. H.; Akis, B. C.; Ayturk, M. E.; Guazzone, F.; Engwall, E. E.; Mardilovich, I. P. *Ind. Eng. Chem. Res.* **2004**, *43*, 2936.
(15) Kamakoti, P.; Sholl, D. S. *Phys. Rev. B* **2005**, *71*, 014301.
(16) Sholl, D. S.; Ma, Y. H. *MRS Bull.* **2006**, *31*, 770.
(17) Greeley, J.; Mavrikakis, M. *Nat. Mat.* **2004**, *3*, 810.
(18) Liu, G.; St. Clair, T. P.; Goodman, D. W. *J. Phys. Chem. B* **1999**, *103*, 8578.
(19) Pope, T. D.; Griffiths, K.; Norton, P. R. *Surf. Sci.* **1994**, *306*, 294.
(20) Olovsson, W.; Bech, L.; Andersen, T. H.; Li, Z.; Hoffmann, S. V.; Johansson, B.; Abrikosov, I. A.; Onsgaard, J. *Phys. Rev. B* **2005**, *72*, 07544401.
(21) Cole, R. J.; Brooks, N. J.; Weightman, P. *Phys. Rev. B* **1997**, *56*, 12178.
(22) Cole, R. J.; Brooks, N. J.; Weightman, P. *Phys. Rev. Lett.* **1997**, *78*, 3777.
(23) Cole, R. J.; Brooks, N. J.; Weightman, P.; Francis, S. M.; Bowker, M. *Surf. Rev. Lett.* **1996**, *3*, 1763.
(24) Andersen, T. H.; Bech, L.; Li, Z.; Hoffmann, S. V.; Onsgaard, J. *Surf. Sci.* **2004**, *559*, 111.
(25) Fernandez-Garcia, M.; Conesa, J. C.; Clotet, A.; Ricart, J. M.; Lopez, N.; Illas, F. *J. Phys. Chem. B* **1998**, *102*, 141.
(26) GandugliaPirovano, M. V.; Kudrnovsky, J.; Scheffler, M. *Phys. Rev. Lett.* **1997**, *78*, 1807.
(27) Kamakoti, P.; Morreale, B. D.; Ciocco, M. V.; Howard, B. H.; Killmeyer, R. P.; Cugini, A. V.; Sholl, D. S. *Science* **2005**, *307*, 569.
(28) Greeley, J.; Mavrikakis, M. *J. Phys. Chem. B* **2005**, *109*, 3460.
(29) Tierney, H. L.; Baber, A. E.; Sykes, E. C. H. *J. Phys. Chem. C* **2009**, *113*, 7246.
(30) Howard, B. H.; Killmeyer, R. P.; Rothenberger, K. S.; Cugini, A. V.; Morreale, B. D.; Enick, R. M.; Bustamante, F. *J. Membr. Sci.* **2004**, *241*, 207.
(31) Saha, D. K.; Koga, K.; Ohshima, K. *J. Phys.: Condens. Mattter* **1992**, *4*, 10093.
(32) Canzian, A.; Mosca, H. O.; Bozzolo, G. *Surf. Sci.* **2004**, *551*, 9.
(33) Miller, J. B.; Matranga, C.; Gellman, A. J. *Surf. Sci.* **2008**, *602*, 375.
(34) Miller, J. B.; Morreale, B. D.; Gellman, A. J. *Surf. Sci.* **2008**, *602*, 1819.
(35) Jankowiak, J. T.; Barteau, M. A. *J. Catal.* **2005**, *236*, 366.
(36) Linic, S.; Jankowiak, J.; Barteau, M. A. *J. Catal.* **2004**, *224*, 489.
(37) Meunier, I.; Treglia, G.; Gay, J. M.; Aufray, B.; Legrand, B. *Phys. Rev. B* **1999**, *59*, 10910.
(38) Umezawa, K.; Nakanishi, S.; Yoshimura, M.; Ojima, K.; Ueda, K.; Gibson, W. M. *Phys. Rev. B* **2001**, *63*, 035402.
(39) Aufray, B.; Gothelid, M.; Gay, J. M.; Mottet, C.; Landemark, E.; Falkenberg, G.; Lottermoser, L.; Seehofer, L.; Johnson, R. L. *Microsc. Microanal. Microstruct.* **1997**, *8*, 167.
(40) Meunier, I.; Treglia, G.; Legrand, B.; Tetot, R.; Aufray, B.; Gay, J. M. *Appl. Surf. Sci.* **2000**, *162*, 219.
(41) Kresse, G.; Furthmüller, J. *Comput. Mater. Sci.* **1996**, *6*, 15.
(42) Kresse, G.; Hafner, J. *Phys. Rev. B* **1993**, *48*, 13115.
(43) Perdew, J. P.; Chevary, J. A.; Vosko, S. H.; Jackson, K. A.; Pederson, M. R.; Singh, D. J.; Fiolhais, C. *Phys. Rev. B* **1992**, *46*, 6671.
(44) Henkelman, G.; Jonsson, H. *J. Chem. Phys.* **2000**, *113*, 9978.
(45) Henkelman, G.; Uberuaga, B. P.; Jónsson, H. *J. Chem. Phys.* **2000**, *113*, 9901.
(46) Kim, S. Y.; Lee, I.-H.; Jun, S. *Phys. Rev. B* **2007**, *76*, 245408.
(47) Leonardelli, G.; Lundgren, E.; Schmid, M. *Surf. Sci.* **2001**, *490*, 29.
(48) Amar, J. G.; Family, F. *Thin Solid Films* **1996**, *272*, 208.
(49) Dougherty, D. B.; Bondarchuk, O.; Degawa, M.; Williams, E. D. *Surf. Sci.* **2003**, *527*, L213.
(50) Giesen, M.; Dietterle, M.; Stapel, D.; Ibach, H.; Kolb, D. M. *Surf. Sci.* **1997**, *384*, 168.
(51) Giesenseibert, M.; Jentjens, R.; Poensgen, M.; Ibach, H. *Phys. Rev. Lett.* **1993**, *71*, 3521.
(52) Jeong, H. C.; Williams, E. D. *Surf. Sci. Rep.* **1999**, *34*, 171.
(53) Pai, W. W.; Bartelt, N. C.; Reutt-Robey, J. E. *Phys. Rev. B* **1996**, *53*, 15991.
(54) Pai, W. W.; Ozcomert, J. S.; Bartelt, N. C.; Einstein, T. L.; Reutt-Robey, J. E. *Surf. Sci.* **1994**, *309*, 747.
(55) Flores, T.; Junghans, S.; Wuttig, M. *Surf. Sci.* **1997**, *371*, 14.

JP903541K